

**MOMENTUM SPECTROSCOPY OF PHASE
FLUCTUATIONS OF AN ELONGATED BOSE-EINSTEIN
CONDENSATE***

A. ASPECT, S. RICHARD, F. GERBIER, M. HUGBART, J. RETTER, J. H.
THYWISSEN[†] AND P. BOUYER

*Laboratoire Charles Fabry, Institut d'Optique,
Bat. 503, Centre Universitaire
F91403, ORSAY, France
E-mail: alain.aspect@iota.u-psud.fr*

1. Introduction: BEC beyond the ideal case

Degenerate atomic Bose gases provide a remarkable testing ground for the theory of dilute quantum fluids, allowing for an extensive comparison of theory and experiment^{1,2}.

First studies on trapped dilute Bose gases have shown behaviors in good agreement with the predictions for homogeneous ideal Bose gases. With the refinement of experimental techniques, however, it becomes possible to study deviations from the ideal case. We have recently made quantitative studies of such deviations, for two different phenomenon:

- (i) Phase fluctuations in an elongated quasi 1D condensate, that lead to a coherence length smaller than the condensate axial size³.
- (ii) Shift of the critical temperature of condensation due to interactions⁴.

In the context of this series of Conferences On Laser Spectroscopy, where we have so strong traditions, I will concentrate on the first study, since we will see that these measurements involve many methods of "Good Old Spectroscopy", transposed from the world of Lasers and Photon Optics, to the world of Bose-Einstein Condensates and Atom Optics.

*This work is supported by CNRS, Ministère de la Recherche, DGA, EU (Cold Quantum Gases network; ACQUIRE collaboration), INTAS(project 01-0855)

[†]Present address: Department of Physics, 60 St George Street, University of Toronto, Toronto, ON, M5S 1A7, Canada

2. Phase fluctuations in a trapped elongated BEC

Three-dimensional (3D) trapped condensates are predicted to have a uniform phase, extending over the whole condensate, even at finite temperature, and this has been confirmed experimentally^{5,6,7}. In low dimensional systems, however, phase fluctuations are predicted to reduce the spatial coherence length (see ^{8,9} and references therein). This phenomenon also occurs in sufficiently anisotropic 3D samples, where complete phase coherence across the axis (long dimension) is established only below a temperature T_ϕ , that can be much lower than the critical temperature T_c ¹⁰. In the range $T_\phi < T < T_c$, the cloud is a “quasi-condensate”, whose incomplete phase coherence is due to thermal excitations of 1D axial modes, with wavelengths larger than its radial size. Phase fluctuations of quasi-condensates in elongated traps have been observed first in Hannover by Dettmer *et al.*¹¹, who measured the conversion, during free expansion, of the phase fluctuations into ripples in the density profile. Although the conversion dynamics is well understood¹², the measured amplitude of density ripples was found smaller than expected by a factor of two. In Amsterdam, Shvarchuck *et al.*¹³ have used a “focusing” method to show that the coherence length is smaller than the sample size during the formation of a condensate.

3. Production and observation of an elongated BEC in an iron-core electromagnet

Our experimental setup has been described elsewhere¹⁴. Briefly, a Zeeman-slowed atomic beam of ⁸⁷Rb is trapped in a MOT, and after optical pumping into the $F = 1$ state is transferred to a magnetic Ioffe-Pritchard trap created by an iron-core electromagnet. A new design allows us to lower the bias field to a few Gauss and thus to obtain very tight radial confinement¹⁵. Final radial and axial trap frequencies (ω_\perp and ω_z) are respectively 760 Hz and 5 Hz (*i.e.* an aspect ratio of 152). We typically obtain needle-shaped condensates containing around 5×10^4 atoms, with a typical half-length $L \simeq 130 \mu\text{m}$ and radius $R \simeq 0.8 \mu\text{m}$. Since the chemical potential is only slightly larger than the radial vibration quantum, ($\mu_{\text{TF}}/\hbar\omega_\perp \sim 4$), we work at the crossover between the 3D and 1D Thomas-Fermi (TF) regimes^{16,17,18}.

To obtain the number of atoms in the condensate and in the thermal cloud, and the temperature, we make an absorption image after a 20 ms time of flight. The number of atoms, obtained to within 20%, is calibrated from a measurement of the temperature of condensation T_c . The temperature T is extracted from a two-component fit to the absorption images,

yielding the temperature of the thermal cloud fitted by an ideal Bose function with zero chemical potential. In fact, the temperature obtained at the end of the evaporation ramp can be chosen *a priori* to within 20 nK by controlling the final trap depth (final rf frequency, as compared to the one totally emptying the trap, with is checked every five ramps) to a precision of 2 kHz. This provides a high reproducibility which is a real asset for these experiments.

As Shvarchuck *et al.*¹³, we observe strong shape oscillations at the formation of the condensate¹⁹, despite a slow evaporation (less than 100 kHz/s) across T_c . We then hold the condensate for a time of typically 7 seconds in the presence of an rf shield, to damp the axial oscillations enough that they do not affect the Bragg spectra (see below).

4. Measurement of the spatial coherence function by Bragg spectroscopy

The most direct way to measure the spatial coherence function relies on atom interferometry. It turns out, however, that this method demands a high level of shot to shot stability of the interferometer²¹, and we have decided to first use a complementary method, that directly yields the momentum distribution (momentum spectrum) $\mathcal{P}(p_z)$, which is nothing else than the Fourier transform of $C(s)$.

This is analogous to the two complementary methods of “Good Old Spectroscopy”, where one can either measure the temporal correlation function of the light (the so called “Fourier-transform spectroscopy”), or directly obtain the frequency spectrum. It is well known that the second type of method is much easier to implement, because some physical phenomena (as dispersion in dielectric media) or “simple” devices (as diffraction gratings) are able to separate frequency components whose weight can be directly measured. The methods yielding directly the spectrum were in fact the only ones that were used for centuries, until stable and reliable enough interferometers became available.

In our problem of Atom Optics, it turns out that we also have a method that directly yields the momentum spectrum: this is “Bragg Spectroscopy”^{6,22}. Our momentum distribution measurement is based on four-photon velocity-selective Bragg diffraction. In this process, atoms are extracted out of the condensate by interaction with a moving standing wave, formed by two counter-propagating laser beams with a relative detuning δ . In a wave picture, this can be interpreted as a (second order)

Bragg diffraction of the atomic matter waves off the grating formed by the light standing wave, and it is therefore resonant only for a given atomic de Broglie wavelength, or equivalently for a given value of the atomic momentum. The number of extracted atoms is therefore proportional to the density of probability of that particular value of the momentum. Writing the Bragg condition of diffraction off a thick grating, one finds that the momentum component resonantly diffracted out of the condensate depends on the velocity of the light standing wave, and therefore on the detuning δ , according to

$$p_z = M(\delta - \delta\omega_R)/(2k_L), \quad (1)$$

with $\omega_R = \hbar k_L^2/(2M)$, M the atomic mass, and $k_L = 2\pi/\lambda$ ($\lambda = 780.02$ nm). By varying the detuning δ between the counter-propagating laser beams that make the moving standing wave, and measuring the fraction of diffracted atoms *vs.* δ , one can build the momentum distribution spectrum.

The stability of the differential frequency δ determines the spectral resolution, and must be as good as possible. The optical setup is as follows. A single laser beam is spatially filtered by a fiber optic, separated into two arms with orthogonal polarizations, frequency shifted by two independent 80 MHz acousto-optic modulators, and recombined. The modulators are driven by two synthesizers stable to better than 1 Hz over the typical acquisition time of a spectrum. The overlapping, recombined beams are then sent through the vacuum cell, parallel (to within 1 mrad) to the long axis of the trap, and retro-reflected to obtain two standing waves with orthogonal polarizations, moving in opposite directions. To check the differential frequency stability, we have measured the beat note between the two counter-propagating beams forming a standing wave. The average over ten beat notes had a half-width at half-maximum (HWHM) of 216(10) Hz for a 2 ms pulse²³.

5. Axial Bragg spectrum of an elongated condensate

The following experimental procedure is used to acquire a momentum spectrum. At the end of forced evaporative cooling, the radio frequency knife is held fixed for about 7 s to allow the cloud to relax to equilibrium (see above). The magnetic trap is then switched off abruptly, in roughly 100 μ s, and the cloud expands for 2 ms before the Bragg lasers are pulsed on for 2 ms. The lasers are tuned 6.6 GHz below resonance to avoid Rayleigh scat-

tering, and the laser intensities (about 2 mW/cm^2) are adjusted to keep the diffraction efficiency below 20%.

We take the Bragg spectrum after expansion rather than in the trap to overcome two severe problems. First, in the trapped condensate, the mean free path (about $10 \mu\text{m}$) is much smaller than its axial size of $260 \mu\text{m}$, so that fast Bragg-diffracted atoms would scatter against the cloud at rest²⁵. Second, the inhomogeneous mean field broadening⁶ would be of the order of 300 Hz, *i.e.* larger than our instrumental resolution. By contrast, after 2 ms of free expansion, the peak density has dropped by two orders of magnitude²⁶, and both effects become negligible. One may wonder whether this 2 ms expansion doesn't affect the momentum distribution we want to study. In fact, the phase fluctuations do not significantly evolve in 2 ms, since the typical timescale for their complete conversion into density ripples varies from 400 ms to 15 s for the range of temperatures we explore²⁷. Also, the mean field energy is released almost entirely in the radial direction, because of the large aspect ratio of the trap²⁶, and contributes only about 50 Hz of Doppler broadening in the axial direction. The only perturbation due to the trap release seems to be small axial velocity shifts (around $100 \mu\text{m/s}$) attributed to stray magnetic gradients that merely displace the spectra centers.

After application of the Bragg pulses, we wait for a further 20 ms to let the diffracted atoms separate from the parent condensate, and take an absorption image. Diffraction efficiency is defined as the fraction of atoms in the secondary cloud. We repeat this complete sequence typically five times at each detuning, and we average the diffraction efficiency for this particular value of the detuning. Repeating this process at various values of the detuning (typically 15), we plot the diffraction efficiency *vs.* δ , and obtain an "elementary spectrum".

As shown on Fig. 1a, an elementary spectrum at a given temperature still shows a lot of noise. To average out this noise, we have taken many elementary spectra at the same temperature (between 10 and 40), but during different runs (on different days). We have also varied the hold time (of about 7 s, see above) over a range of 125 ms, to average on possible residual shape oscillations. We then take all the spectra corresponding to the same temperature, and we reduce them to the same surface, background, and center, and superpose them²⁴.

Fig. 1b shows the result of such a data processing, at a temperature well above T_ϕ , *i.e.* for a case where the broadening due to phase fluctuations is expected to dominate over the instrumental resolution. The

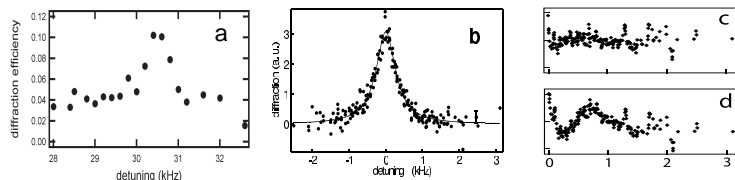


Figure 1. **Bragg spectrum of an elongated BEC** at $T = 261(13)$ nK, corresponding to $T/T_\phi = 20(2)$. **(a)** Elementary spectrum (*i.e.* diffraction efficiency *vs.* relative detuning of the Bragg lasers) corresponding to 75 diffraction efficiency measurements made at the same temperature, but at various detunings (see text). Measurements at the same detuning (typically 5) are averaged. **(b)** Averaged spectrum, obtained by averaging 12 (recentered and rescaled, see text) elementary spectra. A typical statistical error bar is shown. This spectrum is the superposition of 12 “elementary spectra”, as described in the text. The solid line is a Lorentzian fit, giving a half-width at half-maximum (HWHM) of $316(10)$ Hz. **(c)** and **(d)** show respectively the (folded) residuals of a Lorentzian and of a Gaussian fit to the above spectrum.

width ($316(10)$ Hz, HWHM) is definitely larger than the resolution (less than $216(10)$ Hz, HWHM). Moreover, it is clear by simple visual inspection, and confirmed by examining the residuals of fits (see Fig. 1c and d) that the profile shape is definitely closer to a Lorentzian than to a Gaussian. Such a shape is in contrast to the gaussian-like profile expected for a pure condensate^{6,20}, and it is characteristic of large 1D phase fluctuations²⁷, which result in a nearly exponential decay of the correlation function.

6. Results. Comparison to theory

Bragg spectra have been taken at various temperatures between T_ϕ and T_c . Using a Lorentzian fit, we extract a measured half-width $\Delta\nu_M$ for each temperature, and plot it (Figure 2a) *vs.* $\Delta\nu_\phi$, a parameter convenient to compare to the theory. That parameter can be directly expressed as a function of the number of atoms and the temperature, and theory predicts that the ideal spectrum half-width should be proportional to $\Delta\nu_\phi$, with a multiplying factor α , depending on the density profile, of the order of 1 ($\alpha = 0.67$ in our case)^{27,3}. In fact, since our spectral resolution is limited, the measured spectrum width $\Delta\nu_M$ results from a convolution of the ideal Lorentzian profile by the resolution function, that we assume to be a Gaussian, of half-width w_G . The measured spectrum is then expected to be a Voigt profile, whose shape can hardly be distinguished from a Lorentzian in our range of parameters, but with a width (HWHM) $\alpha\Delta\nu_\phi/2 + \sqrt{w_G^2 + (\alpha\Delta\nu_\phi)^2/4}$. We use that expression to fit the data of Fig. 2a, taking α and w_G as free parameters. We find $w_G = 176(6)$ Hz, and $\alpha = 0.64(5)(5)$. The first uncer-

tainty quoted for α is the standard deviation of the fit value. The second results from calibration uncertainties on the magnification of the imaging system and on the total atom number, which do not affect w_G . We note first that the fitted value of w_G is slightly smaller than 216 Hz, as it should be²³. The agreement of the measured value of α with the theoretical value 0.67, to within the 15% experimental uncertainty, confirms quantitatively the temperature dependence of the momentum width predicted in Ref. ¹⁰.

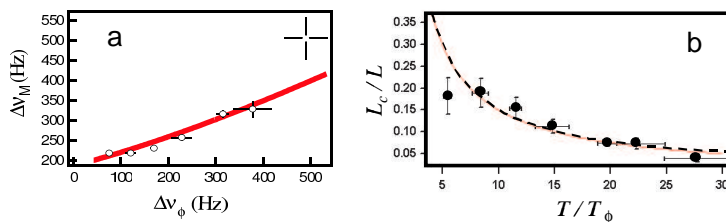


Figure 2. **Momentum distribution width and coherence length for $T/T_\phi > 1$.** (a) Half-widths at half-maximum $\Delta\nu_M$ of the experimental Bragg spectra versus the parameter $\Delta\nu_\phi$ (see text). The solid line is a fit assuming a Voigt profile with a constant Gaussian resolution function. (b) Coherence length L_c (divided by the condensate half size L) vs. temperature (divided by T_ϕ). The coherence length is obtained after deconvolution from the resolution function.

Conclusion

We have shown that the momentum spectrum of an elongated condensate at a temperature smaller than T_c but larger than T_ϕ has a Lorentzian shape, in contrast with the Gaussian shape of a "normal" condensate. That shape, as well as the measured broadening, agree quantitatively with the predictions for a phase fluctuating condensate. The coherence lengths corresponding to the spectrum widths are smaller than the condensate axial size (Fig. 2b). It would be interesting to also measure the coherence length for temperatures approaching T_ϕ , to study how coherence develops over the whole condensate. Since this corresponds to smaller and smaller momentum widths, the method presented here is not well adapted, and an interferometric measurement directly yielding the spatial correlation function at large separations would be a method of choice. Such measurements require a large path difference of the interferometer, and the stability of the interferometer is a crucial issue. We are currently working in that direction.

References

1. F. Dalfovo, S. Giorgini, L. P. Pitaevskii, and S. Stringari, *Rev. Mod. Phys.* **71**, 436 (1999).
2. E. A. Cornell and C. E. Wieman *Rev. Mod. Phys.* **74**, 875-893 (2002); W. Ketterle *Rev. Mod. Phys.* **74**, 1131-1151 (2002).
3. R. Simon *et al.*, *Phys. Rev. Lett.* **91**, 010405 (2003).
4. F. Gerbier *et al.*, cond-mat/0307188.
5. E. W. Hagley *et al.*, *Phys. Rev. Lett.* **83**, 3112 (1999).
6. J. Stenger *et al.*, *Phys. Rev. Lett.* **82**, 4569 (1999).
7. I. Bloch, T. W. Hänsch, T. Esslinger, *Nature* **403**, 166 (2000).
8. D. S. Petrov, G. V. Shlyapnikov, J. T. M. Walraven, *Phys. Rev. Lett.* **85**, 3745 (2000).
9. J. O. Andersen, U. Al Khawaja, H. T. C. Stoof, *Phys. Rev. Lett.* **88**, 070407 (2002); D. L. Luxat, A. Griffin, cond-mat/0212103; C. Mora, Y. Castin cond-mat/0212523.
10. D. S. Petrov, G. V. Shlyapnikov, J. T. M. Walraven, *Phys. Rev. Lett.* **87**, 050404 (2001).
11. S. Dettmer *et al.*, *Phys. Rev. Lett.* **87**, 160406 (2001); D. Hellweg *et al.*, *Appl. Phys. B* **73**, 781 (2001).
12. H. Kreutzmann *et al.*, cond-mat/0201348.
13. I. Shvarchuck *et al.*, *Phys. Rev. Lett.* **89**, 270404 (2002).
14. B. Desruelle *et al.*, *Phys. Rev. A* **60**, R1759 (1999).
15. V. Boyer, thèse de doctorat, Institut d'Optique-Université Paris VI2000.
16. A. Görlitz, J. M. Vogels, A. E. Leanhardt, C. Raman, T. L. Gustavson, J. R. Abo-Shaer, A. P. Chikkatur, S. Gupta, S. Inouye, T. Rosenband, and W. Ketterle, *Phys. Rev. Lett.* **87**, 130402 (2001).
17. F. Schreck, L. Khaykovich, K. L. Corwin, G. Ferrari, T. Bourdel, J. Cubizolles, and C. Salomon *Phys. Rev. Lett.* **87**, 080403 (2001).
18. M. Greiner, I. Bloch, O. Mandel, T. W. Hänsch, and T. Esslinger, *Phys. Rev. Lett.* **87**, 160405 (2001).
19. F. Gerbier *et al.*, cond-mat/0210206.
20. F. Zambelli, L. Pitaevskii, D. M. Stamper-Kurn, S. Stringari, *Phys. Rev. A* **61**, 063608 (2000).
21. Note however that recently the Hanover group has succeeded in such a measurement, and obtained results analogous to ours: *D. Hellweg et al.*, *Phys. Rev. Lett.* **91**, 010406 (2003).
22. J. Steinhauer, R. Ozeri, N. Katz, N. Davidson, *Phys. Rev. Lett.* **88**, 120407 (2002).
23. Since supplementary mirrors must be added to perform this measurement, the result is an upper limit to the linewidth of δ .
24. S. Richard, Thèse de l'université d'Orsay (2003)
25. A. P. Chikkatur *et al.*, *Phys. Rev. Lett.* **85**, 483 (2000).
26. Y. Castin, R. Dum, *Phys. Rev. Lett.* **77**, 5315 (1996); Yu. Kagan, E. L. Surkov, G. V. Shlyapnikov, *Phys. Rev. A* **55**, R18 (1997).
27. F. Gerbier *et al.*, *Phys. Rev. A* **67**, 051602(R) (2003) .